A PARAMETERIZED SIMULATION OF DOPPLER LIDAR

by

David B. Chester

A thesis submitted in partial fulfillment
of the requirements for the degree

of

MASTER OF SCIENCE

in

Electrical Engineering

Approved:

Scott E. Budge, PhD Major Professor	Jacob Gunther, PhD Committee Member
Charles M. Swenson, PhD Committee Member	Mark R. McLellan, PhD Vice President for Research and Dean of the School of Graduate Studies

UTAH STATE UNIVERSITY
Logan, Utah

2017

CONTENTS

LIST OF FIGURES

CHAPTER 1

LadarSIM

LadarSIM is a robust parameterized tool for simulating lidar systems, which has been developed at Utah State University's Center for Advanced Imaging Ladar (CAIL) since 2003 [1, 2]. LadarSIM was originally developed to simulated pulsed time-of-flight lidar systems and has the flexibility to simulate a wide range of these systems by simulating parameterized lidar transceiver, focal plane arrays, and pointing/scanning systems, as well as the interaction of the lidar with a simulated 3D scene.

CHAPTER 2

Frequency Modulated Continuous Wave Detection

2.1 FMCW Radar

The theory behind Frequency Modulated Continuous Wave (FMCW) detection will be explored in this section following the development of Brooker [3]. Booker's development focuses on FMCW radar, but the same theory applies to FMCW lidar by making the appropriate changes in the system hardware. For example, the antennae would be replaced with a telescope etc.

2.1.1 Basic Principles

FMCW detection refers to a radar/lidar system in which a continuous wave of known frequency is modulated in amplitude, transmitted, and the reflected signal is detected. A continuous wave radar in which a single microwave oscillator serves as both the transmitter and local oscillator (LO) is, generally speaking, a homodyne radar. Frequency modulated continuous waveform (FMCW) radar systems often leverage a homodyne architecture.

An FMCW radar uses a continuous wave signal which is modulated in amplitude over a range of frequencies creating a linear chirp. This chirped signal is radiated to the target and an echo returns after time T_p, which is the time it takes for the signal to reach the target and reflected energy to return to the antennae. Figure 2.1 illustrates a chirped signal, shown with a solid line, and the return signal delayed by T_p, shown with a dashed line. In this figure f_b refers to the difference in frequency of the two signals at a given time.

It is clear that the distance to the target can be calculated with T_p. In an FMCW system T_p is determined by measuring the beat frequency f_b. To do this a portion of the signal produced by the LO is mixed with the returned echo producing f_b. A signal chirped in frequency can be expressed as

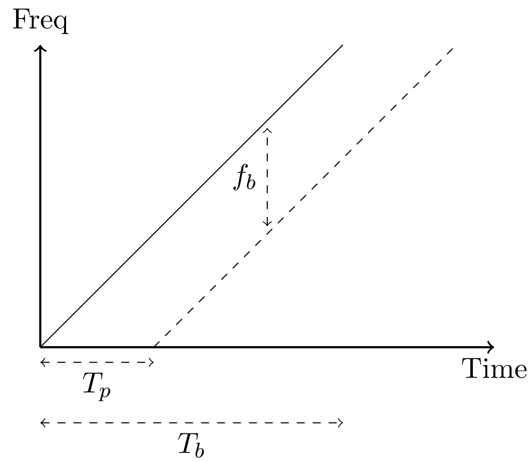

Fig. 2.1: Transmit and Receive Doppler Shift

$$v_{fm}(t) = A_c cos[\omega_c t + \frac{A_b}{2} t^2]. \tag{2.1}$$

Where A_b is a constant of proportionality between the change in frequency over the chirp or chirp slope, ω_b, and the chirp time; such that $\omega_b = A_b t$. The mixture of the transmitted and received signals can be expressed as

$$v_{fm}(t - T_p) v_{fm}(t) = A_c^2 cos[\omega_c t + \frac{A_b}{2} t^2] cos[\omega_c (t - T_p) + \frac{A_b}{2} (t - T_p)^2]. \tag{2.2}$$

This simplifies to

$$v_{out}(t) = A_c^2 (cos[(2\omega_c - A_b T_p)t + A_b t^2 + (\frac{A_b}{2} T_p^2 - \omega_c T_p)] + cos[A_b T_p t + (\omega_c T_p - \frac{A_b}{2} T_p^2)]). \tag{2.3}$$

It is desirable to isolate the second term in Eq 2.3 because it is the the beat signal. The first cosine term is an FM chirp at about twice the carrier frequency and is in most cases conveniently filtered out because it is above the cutoff frequency of the receiver components. To obtain the f_b from the beat signal the phase term is differentiated with time,

$$f_b = \frac{1}{2\pi}\frac{d}{dt}[A_b T_b t + (\omega_c T_p - \frac{A_b}{2}T_p^2)], \tag{2.4}$$

resulting with

$$f_b = (\frac{A_b}{2\pi})T_p. \tag{2.5}$$

2.1.2 FMCW Detection

As discussed above, the most common way to obtain the beat frequency, f_b, is to take the product of the transmitted chirp signal and the received signal and filter to isolate the constant frequency beat. The Fast Fourier Transform (FFT) is the most common method of spectral analysis employed in FMCW radar to measure f_b.

Given a chirp duration, T_b(s), and assuming that $T_b \gg T_p$, the maximum resolution of the beat frequency is $2/T_b$(Hz). Figure 2.1 shows a chirp which meets that criterion. The resolution bandwidth of a signal, δf_b, is commonly defined between its 3 dB points. For the truncated chirp case δf_b coincides with a region of width $1/T_b$ centered on f_b, as shown in figure 2.2.

The chirp bandwidth is the total change in frequency for the chirp, Δf. Clearly the slope of the chirp is the chirp bandwidth divided by the chirp time, $\Delta f/T_b$. Eq 2.5 can then be restated

$$f_b = (\frac{A_b}{2\pi})T_p = \frac{\Delta f}{T_b}T_p. \tag{2.6}$$

Intuitively T_p is the round trip time from the antennae to the target and back

$$T_p = 2\frac{2R}{c}, \tag{2.7}$$

where c is the speed of light. The classical FMCW formula is obtained by substituting into eq 2.6:

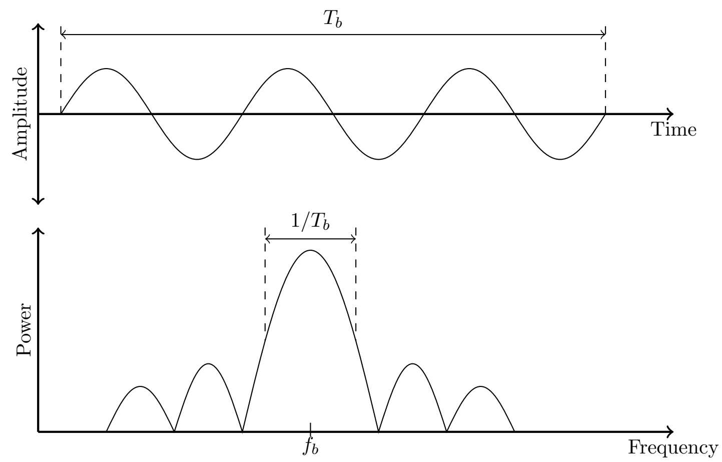

Fig. 2.2: Spectrum of the truncated sinusoidal signal output by an FMCW radar.

$$f_b = \frac{\Delta f}{T_b}\frac{2R}{c}, \tag{2.8}$$

relating the beat frequency to the range. Solving for range yields

$$R = \frac{T_b c}{2\Delta f} f_b. \tag{2.9}$$

Eq 2.9 relates range to beat frequency. The same equation can be used to related range resolution δf and chirp bandwidth:

$$\delta R = \frac{T_b c}{2\Delta f}\delta f = \frac{c}{2\Delta f}. \tag{2.10}$$

Where the frequency resolution $deltaf$ is approximately equal to $1/T_b$.

2.1.3 Doppler Effect in FMCW

So far the development in this section has assumed a stationary radar and target. The case where the radar, the target, or both are moving will now be examined. The Doppler effect describes the change in observed and transmitted frequencies when the distance between the two is changing. The relationship between the transmitted frequency, f_c, and the received frequency, f_r can be expressed

$$f_r = \frac{c + v_t}{c + v_s} f_c. \tag{2.11}$$

Where v_t is the velocity of the target and v_s is the velocity of the source. From eq 2.11 it is simple to obtain an equation for the change in frequency, Δf in relation to the difference in velocity of the source and target, Δv:

$$\Delta f = \frac{c\Delta v}{c} f_s. \tag{2.12}$$

For the following development the radial velocity, v_r(m/s), will represent the velocity term causing the Doppler effect. Modifying eq 2.1 to incorporate the Doppler shift of the echo signal yields:

$$v_{fm}(t - T_p) = A_c cos[\omega_c(t - T_p) + \frac{A_b}{2}(t - T_p)^2 - \frac{2v_r}{c}\omega_c(t - T_p)]. \tag{2.13}$$

The new beat frequency then is the same as derived in eqs 2.5 and 2.6 shifted by the Doppler frequency, f_d:

$$f_b = \frac{2v_r}{c} f_c - \frac{A_b}{2\pi} T_p = f_d - \frac{A_b}{2\pi} T_p. \tag{2.14}$$

For a chirp with positive A_b, an up-chirp, the beat frequency will be the difference between the Doppler frequency f_d and the beat frequency caused by the echo time or range frequency f_r. For a down-chirp, a negative slope, the beat frequency will be the sum of the Doppler frequency and the range frequency. In many radar applications it can be assumed that the Doppler frequency is lower than the range frequency leading to eqs 2.15 and 2.16. If f_d ¿ f_b, as is frequently the case in Lidar, the roles of f_d and f_b are reversed.

$$f_{bUp} = f_b - f_d \tag{2.15}$$

$$f_{bDown} = f_b + f_d \tag{2.16}$$

By using a triangle waveform the sum and difference frequencies can be obtained to isolated range and velocity measurements. Fig 2.3 illustrates the Doppler effect on an FMCW waveform transmitting a triangle wave pattern. Expressions for f_r and f_d can be obtained by averaging and differencing eqs 2.15 and 2.16:

$$f_r = \frac{f_(b(up)) + f_(b(down))}{2}, \tag{2.17}$$

$$f_d = \frac{f_(b(up)) - f_(b(down))}{2}. \tag{2.18}$$

The sign of f_d is determined by the direction of motion. If the range is getting smaller f_d will be positive and if the range is getting larger f_d will be negative.

2.2 FMCW Lidar Architecture

The above section explored the basic functionality of FMCW radar. These basic concepts can be used to develop an FMCW lidar system. This change leads to very few alterations to the equations in section 2.1, most notably that in many lidar systems f_d will be greater than f_b. In this section a number of detection architectures for FMCW lidar will be examined. Adany et al. provide and analysis of direct detection, heterodyne detection, as well as their proposed simplified homodyne detection [4,5] which will serve as the primary source of information in this section.

2.2.1 Direct Detection

In an FMCW direct detection scheme, the signal from the modulation waveform generator is split. Part of the signal is used to modulate the amplitude of the laser, which is then amplified and sent to the telescope. The returning light is captured through the same telescope and converted into an electrical signal via a photo detector. The other part of the modulation signal is then mixed with the electrical signal from the detected returning light to perform de-chirping. An FFT is then taken on the de-chirped signal to find the beat frequency and the range information. The returning signal is weak so the signal to

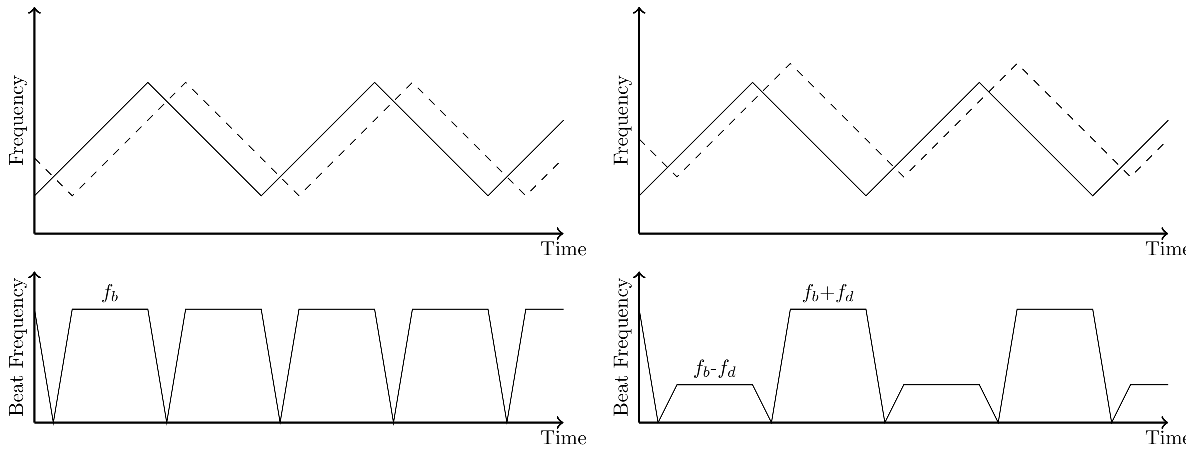

Fig. 2.3: Doppler Effect on FMCW radar.

noise ratio (SNR) at the output of the photodiode is primarily limited by thermal noise. Considering only thermal noise leads to the following expression for the maximum SNR:

$$SNR_{dir} \approx \frac{2\Re^2 P_{sig}^2}{\frac{4kTB_e}{R_L}}. \tag{2.19}$$

Where $\Re$ is the photodiode responsivity, P_{sig} is the optical power of the received sigal, k is Planck's constant, T is the absolute temperature, B_e is the electrical bandwidth, and R_L is the load resistance. Analysis of eq 2.19 shows that for every dB reduction in the return signal power the SNR is reduced by 2 dB. This disadvantage leads to very quick degradation of the performance of a lidar system using direct detection as range increases.

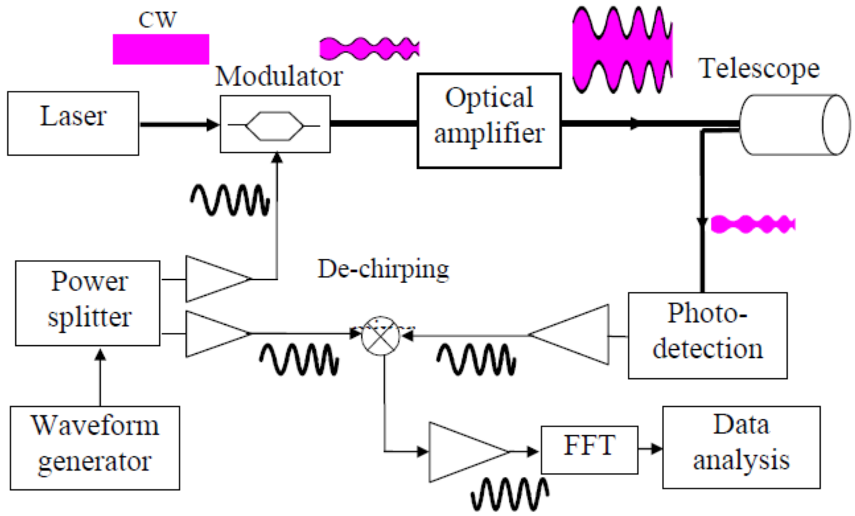

Fig. 2.4: Direct detection architecture

2.2.2 Coherent Heterodyne Detection

In coherent heterodyne detection the laser is split into two signals. One of these signals is modulated by the chirp waveform sent through an optical amplifier and out of the telescope. The other part of the the laser beam is used as the optical local oscillator. This LO signal is then shifted by an acousto-optic modulator to serve as the intermediate frequency (IF) for coherent heterodyne detection. The IF is optically mixed with the returning signal from the telescope, the output of the optical mixer is fed into a balanced photodiode. The photodiode rejects the direct detection component. The output of the photodiode is filtered to isolate the heterdyne IF signal which is detected by an envelope detector. The IF signal is then mixed with the modulation waveform for dechirping. An FFT is then performed on the dechirped signal to recover the beat frequency.

Optically mixing the returned signal with the LO helps mitigate the thermal noise in the photodiode. But because the strong optical LO, the SNR is limited by the shot noise. The theoretical best SNR for a coherent heterodyne lidar is

$$SNR_{het} \approx \frac{\Re P_{sig}}{2qB_e}. \tag{2.20}$$

In this equation q is the electron charge. In coherent heterodyne detection the SNR is linearly proportional to the optical power, making it more suitable for low power operation. The most significant disadvantage of coherent heterodyne detection is its complexity. The IF must be set much higher than the baseband, often in the GHz. This necessitates high speed optical detection and radio frequency (RF) processing circuitry. The IF envelope detection process mixes the signal with RF noise which can further limit the SNR. Because of this the theoretical SNR defined in eq 2.20 has not been obtained in a coherent heterodyne implementation [6].

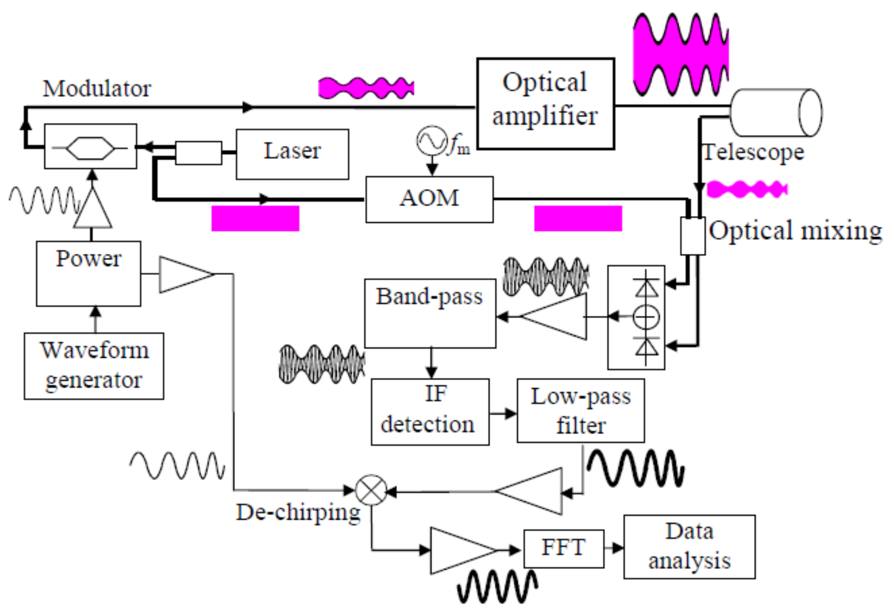

Fig. 2.5: Coherent heterodyne detection architecture

2.2.3 Homodyne Self-Chirped Detection

The homodyne self-chirped architecture was developed to maintain the receiver sensitivity obtained from coherent heterodyne detection while minimizing complexity. In this simplified homodyne detection scheme the laser is modulated by the chirp waveform then split in two. One part of the modulated laser is amplified and sent out the telescope, the other is used as the LO. The returned laser signal is mixed with the LO via a 2x2 optical coupler the output of which is fed into a balanced photodetector. Because the LO is modulated with the same waveform as the transmitted laser, the optical mixing performs both optical detection and RF de-chirping. This reduces the amount of RF noise which is introduced to the detection signal. Performing an FFT on the output of the photodetector yields the beat frequency.

The simplification of the signal path in the homodyne self-chirped architecture results in a practical SNR closer to the theoretical SNR in eq2.20 than the practical SNR of the coherent heterodyne architecture.

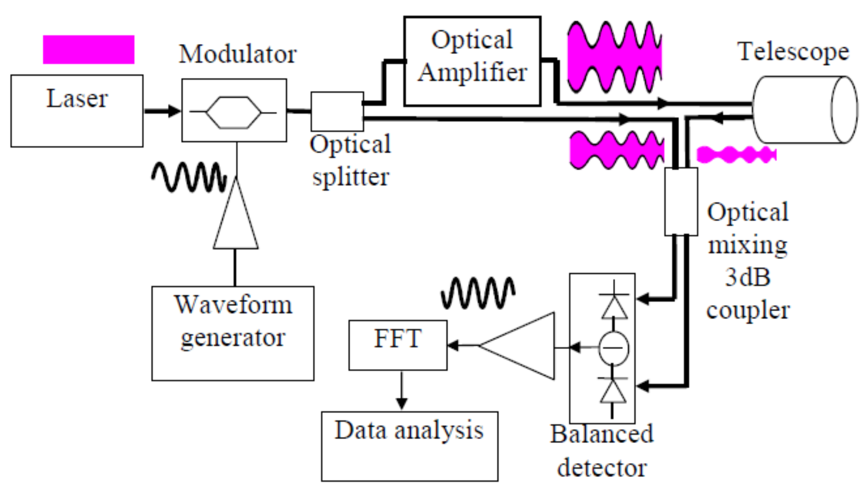

Fig. 2.6: Homodyne self-chirped detection architecture

REFERENCES

[1] S. Budge, B. Leishman, and R. Pack, "Simulation and modeling of return waveforms from a ladar beam footprint in usu ladarsim," pp. 62 140N–62 140N–10, 2006. [Online]. Available: http://dx.doi.org/10.1117/12.666404

[2] K. D. Neilsen, S. E. Budge, R. T. Pack, R. R. Fullmer, and T. D. Cook, "Design and validation of the eyesafe ladar testbed (elt) using the ladarsim system simulator," pp. 73 230B–73 230B–7, 2009. [Online]. Available: http://dx.doi.org/10.1117/12.818856

[3] G. Brooker, "Introduction to sensors for ranging and imaging," 2009.

[4] P. Adany, C. Allen, and R. Hui, "Chirped lidar using simplified homodyne detection," *Journal of Lightwave Technology*, vol. 27, no. 16, pp. 3351–3357, Aug 2009.

[5] P. Adany, *Simplified homodyne detection for FM chirped lidar.* ProQuest, 2007.

[6] C. Allen, Y. Cobanoglu, S. K. Chong, and S. Gogineni, "Performance of a 1319 nm laser radar using rf pulse compression," in *IGARSS 2001. Scanning the Present and Resolving the Future. Proceedings. IEEE 2001 International Geoscience and Remote Sensing Symposium (Cat. No.01CH37217)*, vol. 3, 2001, pp. 997–999 vol.3.